THE JOURNAL OF PHYSICAL CHEMISTRY B

Article

pubs.acs.org/JPCB

Distance Measurements on Orthogonally Spin-Labeled Membrane Spanning WALP23 Polypeptides

Petra Lueders,[†] Heidrun Jäger,[‡] Marcus A. Hemminga,[‡] Gunnar Jeschke,[†] and Maxim Yulikov*[,†]

[†]Laboratory of Physical Chemistry, ETH Zurich, Switzerland

[‡]Laboratory of Biophysics, Wageningen University, Wageningen, The Netherlands

Supporting Information

ABSTRACT: EPR-based Gd(III)−nitroxide distance measurements were performed on a series of membrane-incorporated orthogonally labeled WALP23 polypeptides. The obtained distance distributions were stable upon the change of detection frequency from 10 GHz (X-band) to 35 GHz (Q-band). The α-helical pitch of WALP23 polypeptide could be experimentally observed, despite the flexibility of the two spin labels. The spectroscopic properties of Gd(III) ions and nitroxide radicals allow detecting both types of paramagnetic species selectively in different EPR experiments. In particular, this spectroscopic selectivity allows for supplementing Gd(III)−nitroxide distance measurements with independent checks of polypeptide aggregation and with measurements of the local environment of the nitroxide spin labels. All mentioned additional checks do not require preparation of further samples, as it is the case in the experiments with pairs of identical nitroxide spin labels.

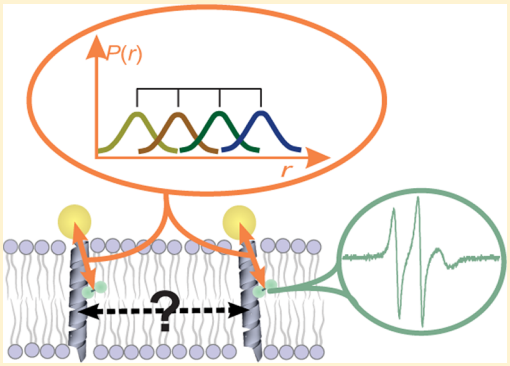

1. INTRODUCTION

Pulse double electron−electron resonance (DEER or PELDOR)[1,2] and related electron dipolar spectroscopy techniques[3−5] are attracting growing attention as powerful tools for obtaining structural information in the nanometer range. Recent DEER experiments on "spectroscopically orthogonal" spin pairs, consisting of Gd(III) centers and nitroxide radicals,[6] have revealed the potential of this combination of spin centers for distance measurements in macromolecules and other nanoobjects. The differences in the optimal microwave power levels and relaxation properties of the two types of paramagnetic centers allow for nearly perfect selective detection of each type of center.[6]

In general the use of high-spin centers in the DEER experiment may cause a problem, because the excitation of more than one electron transition for high-spin centers and the interplay between zero-field splitting (ZFS) and electron Zeeman (EZ) terms in the spin Hamiltonian can create strong distortions of obtained dipolar frequencies and thus of the obtained distances.[7] Surprisingly, for the case of Kramers Gd(III) ions and for the particular distributions of ZFS parameters typical for chelate complexes with this type of ions as well as for the particular experimental settings used in the Gd(III)−nitroxide DEER, the distortions of the obtained distances are between being weak and being negligible.[8] This result opens a broad playground for applying this type of orthogonal labeling in combination with the DEER experiment to obtain structural information in soft matter. As the largest working area of the DEER technique is currently in structural biology,[9−13] it is important to explore the newly developed approach with respect to its biological applications. In particular, DEER techniques are often applied to membrane proteins. Thus, it is of considerable interest to test the new approach on molecules embedded in a lipid bilayer.

The use of two different types of paramagnetic labels allows for new options in DEER such as selective detection of different distances within one spin-labeled macromolecule, macromolecular complex, or other nanoobject.[8,14] Nitroxide radicals are well suited to measure site-specific properties like local polarity, accessibility of the labeled site to solvent molecules, and local packing (via observation of the mobility of a nitroxide label attached with a flexible linker).[11] Such measurements are feasible in the presence of spectroscopically orthogonal spin labels but are usually very difficult if not impossible in the presence of additional nitroxide spin labels at other sites of the macromolecule. Thus, the number of samples that have to be prepared for full characterization can be smaller with an orthogonal labeling approach. These new possibilities are of particular importance for studies of multidomain macromolecular complexes, agglomeration processes, and protein−cofactor or protein−substrate interactions.

The selection of the labeling sites for different types of spin labels must take into account their specific properties. Most existing tags capable to chelate Gd(III) ions were developed for paramagnetic relaxation enhancement or magnetic resonance imaging applications.[15,16] The Gd(III) chelating moieties of

Received: November 15, 2012
Revised: December 20, 2012
Published: February 1, 2013

   dx.doi.org/10.1021/jp311287t | J. Phys. Chem. B 2013, 117, 2061−2068

these tags are usually modestly or strongly hydrophilic, which poses restrictions on the labeling positions. For the important case of membrane-incorporated proteins or polypeptides, the natural choice of the position for Gd(III) tag is thus at a water-exposed region of the macromolecule. The nitroxide spin label can then be attached to the membrane spanning part of the protein or polypeptide. Such a labeling approach is studied here.

In particular, we present an application of Gd(III)−nitroxide DEER to measure distances in orthogonally labeled WALP23 polypeptides and report on the basic features of this approach for membrane-incorporated α-helical domains. A family of WALP polypeptides has been developed to mimic a single α-helical domain of a membrane protein, and a broad range of information on these systems is available.[17−20] An Ln(III)−chelate complex can be introduced to a terminus of such polypeptide via attachment of an additional modified lysine residue. An introduction of a cysteine instead of one of the residues of the core WALP sequence allows for a site-specific labeling with nitroxide radicals.[21] On such a model system one can explore particular details of the Gd(III)−nitroxide distance measurements on membrane-incorporated macromolecules. Note also that DEER in Gd(III)−nitroxide spin pairs can be used as a perfect calibration experiment for developing a relaxation enhancement-based approach for distance measurements.[21,22]

It is worth mentioning that spin labeling requires certain mutations in the studied biomacromolecule. Such mutations could, in principle, induce distortions of the biomolecule's structure. Nevertheless, numerous studies on membrane proteins show that the cysteine mutations are often tolerated by membrane proteins and even by multiple-subunit membrane protein complexes.[11,13] In particular, EPR studies on nitroxide-labeled WALP23 in DOPC bilayers revealed nitroxide label properties consistent with the unbroken α-helical structure of modified WALP23.[23] The paramagnetic labels, containing Gd(III) centers, are used in NMR spectroscopy and typically do not distort the protein structure either.[24,25]

This paper is structured as follows: first we describe sample preparation and experimental details for continuous wave (CW) and pulse EPR measurements, and then we present the nitroxide mobility measurements in the presence of lanthanide centers. The Gd(III)−nitroxide DEER data are presented after this and are supplemented by estimates of ZFS strength for the studied Gd(III) centers, by a discussion of an observed echo reduction effect, and by demonstration of an independent aggregation check with nitroxide−nitroxide DEER. In the Discussion section we compare performance of DEER measurements on Gd(III)−nitroxide pairs and on several other studied spin pairs. Possible orthogonal labeling schemes are briefly discussed.

2. MATERIALS AND METHODS

The samples were prepared according to a previously published procedure.[21] Four WALP23 constructs were synthesized by Pepceutical Limited (Nottingham, UK) by solid-phase synthesis with cysteine at position 7, 11, 15, or 19 for labeling with MTSSL and with a DOTA−lysine derivative (Macrocyclics) at the N-terminus. The selected nitroxide labeling positions approximately correspond to one full turn of an ideal α-helix. The lanthanide-loaded and nitroxide-labeled WALP23-based constructs were incorporated into DOPC bilayers with a peptide-to-phospholipid molar ratio of 1/800. With this mixing ratio the average membrane area per 1 WALP23 peptide was about 280 nm^2, assuming a ∼0.7 nm^2 area per 1 DOPC molecule.[26,27] In our sample preparation procedure, the lanthanide loading was performed before peptide incorporation into lipid vesicles, with a purification step between these two operations.[21] Due to this protocol, and the large thermodynamic and kinetic stability of DOTA−lanthanide complexes,[28] possible formation of complexes between bare lanthanide ions and lipid head-groups[29] can be excluded. Unilamellar vesicles were prepared in a 20 mM Tris-HCl buffer (pH = 7.5). The vesicle size was controlled by extrusion through a filter with a pore size of 400 nm. Bulk concentrations of membrane-incorporated doubly labeled polypeptide in the range 85−260 μM were achieved (Table 1). Complete nitroxide labeling has been confirmed by CW EPR intensity measurements of the spin concentrations and by independent determination of the polypeptide concentration from optical absorption at the wavelength of 280 nm. A loading efficiency of Gd(III) ions into the DOTA moieties close to 100% is expected by analogy to the Dy(III)−nitroxide samples reported previously.[21] Note also that the output of the Gd(III)−nitroxide DEER experiment is not expected to depend on the relative fractions of peptides with and without Gd(III) centers. The only impact of the number of Gd(III)−labeled peptides should be the change of the obtained signal-to-noise ratio. All samples were prepared with an additional removal of O_2 from the lipid bilayer, before shock freezing the samples in liquid nitrogen.[21] The samples were stored in liquid nitrogen between the measurements.

Table 1. Polypeptide Concentrations and Observed DEER Modulation Depths for the Four Studied WALP23 Constructs

nitroxide labeling site	polypeptide concentration[a] (μM)	modulation depth[a] at X-band	modulation depth[a] at Q-band
7	85	0.42	0.31
11	260	0.58	0.41
15	148	0.59	0.44
19	217	0.51	0.42

[a]Concentration error ±20%; modulation depth error estimate: X band ±15%, Q-band ±25%.

The concentration of nitroxide radicals (Table 1) was calculated by recording room temperature (RT) CW EPR spectra, double integrating, and comparing to the corresponding data of a reference nitroxide solution of 300 μM concentration. The nitroxide RT CW spectra for the mobility and for the concentration measurements were recorded at 25 dB attenuation (200 mW full incident microwave power at 0 dB attenuation), with a modulation amplitude of 1 G and a field modulation frequency of 100 kHz. In order to reduce the dielectric losses, the samples were placed into thin glass capillaries (∼0.4 mm inner diameter, BLAUBRAND micropipets). In view of later comparison to relaxation enhancement-based measurements, which will be reported in a separate publication, and in order to test the impact of the magnetic dipolar interaction between lanthanide ions and nitroxide radicals on the shape of nitroxide EPR spectrum, we recorded the nitroxide CW EPR spectra for the samples loaded with different types of lanthanide ions (diamagnetic La(III), paramagnetic Dy(III), and Gd(III); see Figure 1).

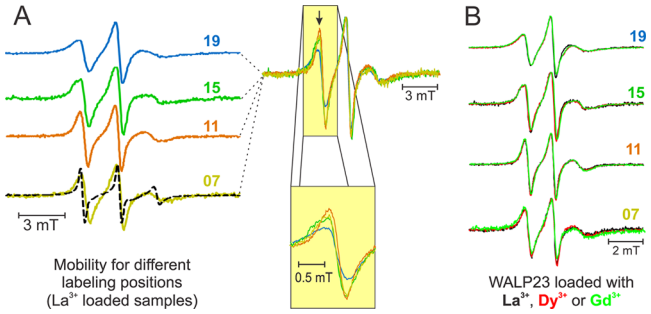

Figure 1. CW EPR spectra of nitroxide radicals attached to doubly labeled WALP23 constructs incorporated into DOPC bilayers. La(III), Gd(III), or Dy(III) ions were loaded into DOTA−lysine, attached to the N-terminus of WALP23 construct (see text). In the subplot (A) nitroxide spectra of La(III)-loaded samples are shown for labeling positions 7 (apple green), 11 (brown), 15 (green), and 19 (blue). Additionally the mobile CW EPR spectrum of an unfolded WALP23 construct dissolved in trifluoroethanol is shown as a dashed black line. In the upper inset an overlay of CW EPR spectra of the four WALP23 constructs with the same color code as in the subplot (A) is presented, and in the lower inset the low-field component of the spectra is magnified to visualize the change of the mobility of nitroxide labels at different positions of WALP23. In the subplot (B) CW spectra for each of the four labeling positions are shown for the samples loaded with La(III) (black), Dy(III) (red), and Gd(III) (light green), to verify the absence of changes in the nitroxide mobility upon changing the loaded lanthanide ion.

The pulse EPR measurements were performed on four Gd(III)-loaded samples. The X-band pulse EPR measurements were performed with a Bruker Elexsys II E680 X/Q-band spectrometer with an ER 4118X-MS3 resonator (split ring resonator, mw frequency 9.3−9.6 GHz, maximum allowed diameter of a cylindrical sample 3 mm). The Q-band measurements were performed with a home-built spectrometer[30] with a rectangular cavity which allows for oversized (up to 3.0 mm outer diameter) samples.[31] The Gd(III)−nitroxide DEER measurements were performed at 10 K. Sample temperature was stabilized with a He-flow cryostat (ER 4118 CF, Oxford Instruments).

The settings for the pump and detection frequencies at X- and Q-band for the Gd(III)−nitroxide DEER experiment are shown in Figure 2. For Gd(III)−nitroxide DEER the offset between pump and detection frequencies was −80 MHz at X-band and −300 MHz at Q-band. The pumping frequency was set close to the center of the resonator mode, because much higher microwave power is required to flip low-spin nitroxide species (S = 1/2) as compared to the high-spin Gd(III)

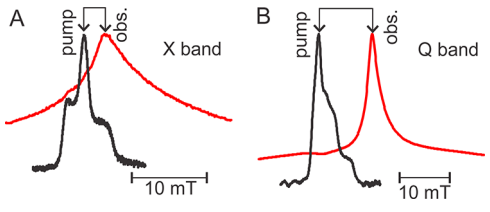

Figure 2. ED EPR spectra of nitroxide radicals (black) and Gd(III) ions (red) detected at optimum settings for each type of species. Spectra were recorded on Gd(III)- and nitroxide-labeled WALP23 sample at X-band (A) and at Q-band (B) at 10 K. In each subplot the positions of pump and observer frequencies for the Gd(III)−nitroxide DEER experiment are shown with arrows.

paramagnetic centers (S = 7/2). Because of this setting and due to the large frequency offset between pump and detection pulses, the sensitivity of Gd(III)−nitroxide DEER at Q-band is dependent on the shape of the wings of the resonator mode. An optimization of the resonator geometry could thus lead to further improvement of sensitivity. As a possible alternative, bimodal resonators[32,33] or a high-power resonator-free approach[34] could be tested in the future for this type of experiments.

In the 4-pulse DEER sequence, all detection pulses were set to a duration of 12 ns both at X- and Q-band. Such short pulses are feasible due to the larger separation of detection and pump frequency, as compared to nitroxide−nitroxide DEER. Sufficient microwave power was available for 12 ns detection pulses even for 300 MHz frequency offset, due to the larger transition moment of the S = 7/2 spin transitions of the Gd(III) ion. At X-band the pump pulse length was 10 ns, whereas at Q-band it was 12 ns. The first interpulse delay was 400 ns in all cases. The second delay time (between the primary echo and the refocusing pulse) was set according to the required length of the DEER trace, which was selected to provide a sufficient range for background correction. Typical measurement time was 15−25 h for X-band measurements and ∼10−30 min for Q-band measurements, depending on the required signal-to-noise ratio. The much shorter measurement time at Q-band frequencies is possible due to an about 1 order of magnitude better sensitivity of the high-power Q-band setup as compared to the best performance commercial X-band machines.[35] A significant sensitivity gain is obtained already with lower power commercial Q-band setups,[36,37] but at these conditions nitroxide radicals can reveal orientation selectivity, which creates problems for the unambiguous distance determination.[35] Another contribution to the sensitivity improvement specific for Gd(III) centers is due to narrowing of the central transition at higher detection frequency.[6,38] Nitroxide−nitroxide DEER experiments were not feasible at temperatures in the range 50−70 K, which is the standard range for nitroxide−nitroxide distance measurements, due to the T_2 relaxation enhancement induced by Gd(III) ions. Instead, the measurements were performed at 10 K, which allowed detecting DEER traces of a length of 1.8 μs. The nitroxide−nitroxide DEER experiments were performed at Q-band with all 12 ns pulses, frequency offset of 100 MHz, and first interpulse delay of 400 ns. The shot repetition time in these measurements was set to 25 ms.

The magnitude of the ZFS interaction, quantified by the axial component $\langle D \rangle$, was estimated by comparing experimental echo-detected (ED) EPR spectra of the Gd(III) ions at X- and Q-band with a series of simulated spectra for different $\langle D \rangle$ (see the Supporting Information for further details). Transverse relaxation of Gd(III) centers was measured at 10 K in a variable-delay Hahn echo experiment (see Supporting Information). The longitudinal relaxation of Gd(III) centers at 10 K allowed for a shot repetition times down to ∼300−400 μs (the used shot repetition times were 330 μs at X-band and 400−1000 μs at Q-band).

Fitting of DEER data was performed with the DeerAnalysis 2009 software.[39] Throughout the observation time, background decay was nearly linear. Hence, background dimensionality could not be determined. Model-free distance distributions were fitted to experimental DEER traces by Tikhonov regularization.[40−42]

dx.doi.org/10.1021/jp311287t | J. Phys. Chem. B 2013, 117, 2061−2068

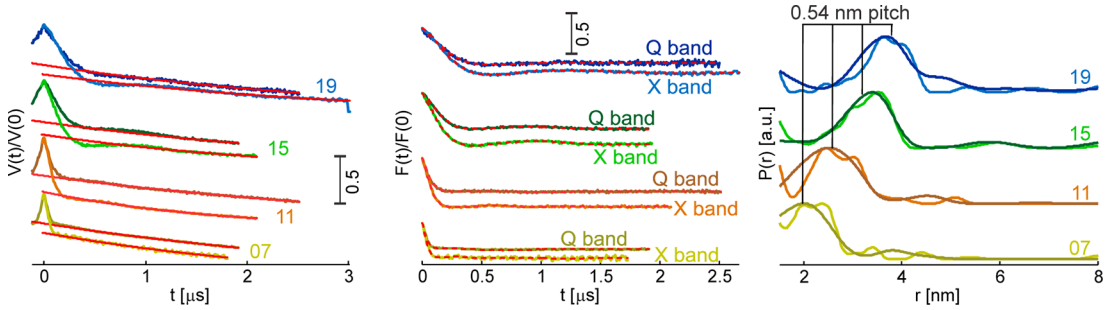

Figure 3. Primary experimental Gd(III)−nitroxide DEER time traces (left subplot), background-corrected form factor signals (central subplot), and obtained distance distributions (right subplot) for the four studied Gd(III)-loaded WALP23 constructs incorporated into DOPC bilayers, with nitroxide label at site 7 (apple green, brass), 11 (brown, dark brown), 15 (green, dark green), and 19 (blue, dark blue). In each pair the darker color corresponds to the Q-band data, and the lighter color corresponds to the X-band data. The background fit functions in the left subplot are shown as solid red curves. The form factor best-fit functions in the central subplot are shown as dashed red curves.

3. RESULTS

Nitroxide radicals can be selectively detected by CW EPR in the presence of Gd(III)- or other lanthanide-containing spin labels, as shown in Figure 1. The EPR spectrum of Gd(III) centers is significantly broader than the corresponding spectrum of nitroxide radicals, and the relaxation of Gd(III) centers is a few orders of magnitude faster than the one of nitroxide radicals. The optimum detection conditions for nitroxide radicals (low incident microwave power, small amplitude of the magnetic field modulation) are thus not suitable for the sensitive detection of Gd(III) centers. For nitroxide−Gd(III) distances below 2 nm, the dipolar interactions between the two paramagnetic species become strong enough to manifest in the change of the EPR line shape of nitroxide radicals. At room temperature this effect is hidden by the increased line width of nitroxide radicals due to Gd(III)-induced relaxation enhancement.[43] At low temperatures this interaction can be potentially detected from CW EPR measurements on nitroxide radicals. In our case such short distances did not contribute largely for any studied sample. This could be seen from the comparison of the nitroxide CW EPR line shapes of WALP23 samples loaded with Gd(III) ions and with diamagnetic La(III) ions. As a result the incorporation of the WALP23 construct into the DOPC bilayer could be monitored indirectly via the change of mobility of the nitroxide label at specific positions in the WALP23 α-helix, and these measurements were insensitive to the presence or absence of paramagnetic Gd(III) ions (Figure 1B).

The mobility is lower for nitroxide spin labels attached closer to the surface of the membrane, and it is higher for the nitroxide labels attached near the middle of WALP23 and thus positioned in the middle of the lipid bilayer.[23] This mobility change correlates with differences in the lipid density through the membrane.[26,27] The mobility of the nitroxide label affects the averaging of the **g**-tensor anisotropy and of the hyperfine anisotropy and thus affects the widths of the three hyperfine components of the nitroxide CW EPR spectrum.[11,12] It is most convenient to observe this effect on the low-field hyperfine component of the nitroxide spectrum due to the fortunate interplay between the intensity, the detection frequency, and the anisotropy contributions for this spectral line, as shown in Figure 1. One can see that this line is broadest for the nitroxide label at site 19, more narrow for the sites 7 and 15, and the narrowest for site 11, which is known to be approximately in the middle of the lipid bilayer.[23] Nitroxides at all four positions in the membrane-incorporated WALP23 construct reveal EPR spectra with much slower motional regime than for the unfolded WALP23 constructs dissolved in TFE (Figure 1A).

The paramagnetic relaxation of Gd(III) ions is much slower than for other paramagnetic Ln(III) ions. As a consequence, the distance between Gd(III) ions and nitroxide radicals can be accessed via the DEER experiment, whereas distances between nitroxide radicals and any other paramagnetic Ln(III) ions should be measured in a relaxation enhancement experiment.[21,22] To prove that the measurements on nitroxide radicals can also be done in the presence of faster relaxing Ln(III) ions, we repeated the CW EPR measurements with Dy(III)-loaded WALP23 samples. The EPR spectrum for each nitroxide labeling site was identical for Dy(III)- and La(III)-loaded samples (Figure 1B). This confirms that relaxation enhancement or dipolar broadening effects on the shape of nitroxide EPR spectrum are insignificant in the studied Ln(III)−nitroxide distance range.

ED EPR spectra of the Gd(III) centers and nitroxide radicals are presented in Figure 2 together with the settings for the pump and detection frequencies in the DEER experiment. The selected positions for the pump and detection frequencies are the same as in our previous works[6,8] and make use of the possibility to perform both pumping and detecting at the maximum intensity of the corresponding EPR lines. The ED EPR spectrum of Gd(III)−DOTA centers is narrower than the one for Gd(III) complexes with DTPA-based chelators.[8] We estimated the *D*-value of the ZFS to be approximately 600 MHz for complexes of Gd(III) ions with DOTA-based ligands (see Supporting Information for further details), whereas for Gd(III)−DTPA complexes *D*-values of about 1500 MHz were estimated.[8,44−46] For Gd(III)−DOTA centers the reduction of the amplitude of the refocused echo upon applying the pump pulse is stronger than previously reported for the Gd(III)−DTPA centers measured with exactly the same pulse settings (see Supporting Information for further details and discussion). This allows us to conclude that the echo reduction observed in Gd(III)−nitroxide DEER experiment cannot be completely explained as a Bloch−Siegert-like phenomenon,[47−49] as a significant contribution to this effect seems to depend on the ZFS parameters of the Gd(III) centers. Possibly, the other proposed echo reduction mechanism,[8] which is specific for high spin systems, is of importance as well.

Results of Gd(III)−nitroxide DEER measurements at X- and Q-band and the obtained distance distributions are shown in Figure 3. The oscillations in the obtained DEER traces decay rather fast, indicating relatively broad Gd(III)−nitroxide

dx.doi.org/10.1021/jp311287t | J. Phys. Chem. B 2013, 117, 2061−2068

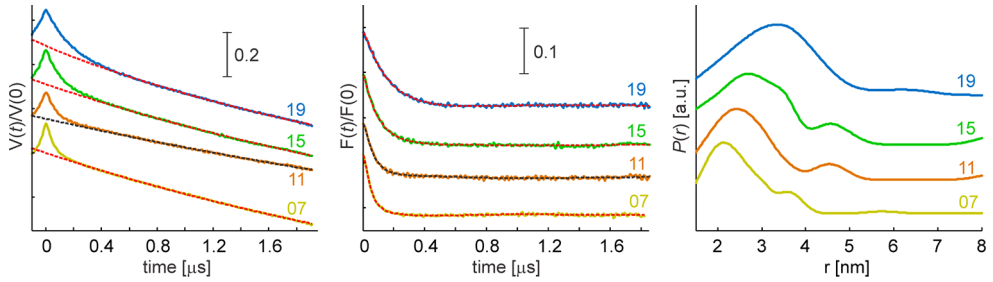

Figure 4. Q-band nitroxide−nitroxide DEER measurements on the four Gd(III)-loaded WALP23 constructs incorporated into the DOPC bilayers, with nitroxide attached at position 7 (apple green), 11 (brown), 15 (green), and 19 (blue). Left subplot, primary time traces with corresponding background fit functions (shown as dashed red curves); central subplot, baseline-corrected form factor signals together with the corresponding best fits (dashed red lines); right subplot, obtained distance distributions.

distance distributions in the samples. The distance distributions obtained from X- and Q-band data are identical within the estimated measurement error. Note that the extracted distance distributions are broad not due to the uncertainty of the distance measurements, which are very precise,[8,39] but due to the real distribution of conformations for the two spin labels in the frozen glassy state. According to established analysis procedures,[9,13,50] the obtained lengths of Gd(III)−nitroxide DEER traces allow for unambiguous detection of distances up to ∼5 nm and for quantitative measurement of the shapes of distance distributions up to $r \sim 3-3.5$ nm, provided that the distance distributions are broad enough, such that the oscillations in the DEER trace decay before its end point. The shift in the mean distance for all four samples agrees with the α-helical pitch of approximately 0.54 nm. The widths of obtained distance distributions reflect the conformational freedom for both nitroxide and Gd(III) labels. The labeling position of the nitroxide provides ample space for reorientation. This is confirmed by the CW EPR line shapes, which are typical for weakly restricted motion and short correlation times.[51] As a result, the flexibility of the Gd(III) label does not broaden the distance distribution much in addition to the impact from the nitroxide label. Clearly, changes of the mean distance of the order of 0.2−0.3 nm can still be monitored in such a system.

Length of DEER traces of up to 3200 ns could be achieved at Q-band (up to 2800 ns at X-band). This parameter is mainly controlled by the transverse relaxation times of Gd(III) centers in the presented system. For a system embedded into a lipid bilayer, these trace lengths compare favorably with the ones that can usually be achieved in nitroxide−nitroxide DEER. Details of the transverse relaxation of Gd(III) centers are given in the Supporting Information.

Modulation depths obtained from the fit of X-band and Q-band Gd(III)−nitroxide DEER traces are shown in the Table 1. The resonator mode profile of the probe head used in Q-band measurements is more sensitive to the shape and dielectric properties of the sample than it is the case for the X-band probe-head, since the oversized sample in the Q-band rectangular resonator is not as well separated from the electric component of the microwave field.[31] Modulation depths in a range between 0.31 and 0.42 were achieved in Q-band measurements. At X-band the resonator mode profile depends less on sample properties and position, and the offset between pump and observer frequencies is lower. Still a distribution of the modulation depth values was obtained for different samples. The DEER modulation depths of X-band traces in the range 0.42−0.59 are in reasonable agreement with the estimates of the inversion efficiency of the 10 ns pump pulse and with the estimate of 100% nitroxide labeling efficiency. The Q-band data are also in line with these estimates, taking into account the somewhat larger error and lower achievable inversion efficiency for the pump pulse, caused by the larger width of the nitroxide spectrum.[35] An additional contribution to lower DEER modulation depths at Q-band comes from somewhat smaller excitation bandwidth of a 12 ns pumping pulses as compared to the 10 ns pumping pulses used at X-band.

For spin-labeled biomacromolecules incorporated into lipid bilayers, enhanced local label concentrations or even aggregation has been identified as an important obstacle for sensitive long-range DEER distance measurements.[52] In particular, intermolecular distance peaks arising from oligomerization or irregular aggregation of the biomacromolecules may be difficult to distinguish from intramolecular distance peaks arising from two labels within the same molecule, if the two labels have identical spectroscopic properties. With an orthogonal labeling approach, part of the intermolecular contributions can be distinguished from the intramolecular contribution by spectral selection.

To demonstrate such spectral selection, we have measured nitroxide−nitroxide DEER on our samples. Because of the labeling approach, we can safely exclude that dipolar modulation in such measurements comes from nitroxide labels within the same peptide molecule. Nevertheless, as is shown in Figure 4, nitroxide−nitroxide DEER oscillations with a depth of about 0.1−0.12 were registered on the studied series of Gd(III)-loaded samples, which implies a certain degree of aggregation (∼20−30%). The nitroxide−nitroxide DEER trace for the sample with nitroxide spin label at site 11 has slower background decay and lower DEER modulation depth as compared to other three samples. This is attributed to a somewhat lower degree of WALP23 aggregation in this sample. Thus, the Gd(III)−nitroxide distance measurements are not completely free from the intermolecular contributions. On the other hand, even at this relatively high level of sample imperfectness, the α-helical pitch is unambiguously seen in the Gd(III)−nitroxide distance distributions (Figure 3). Note also that oscillatory behavior is more pronounced in the Gd(III)−nitroxide DEER traces, and the distance distributions are correspondingly narrower.

4. DISCUSSION

We demonstrated that both at X-band and at Q-band the Gd(III)−nitroxide DEER experiment allows to measure distances on WALP23 polypeptide samples with concentrations typical for DEER applications to biomacromolecules in general and membrane proteins in particular. No strong indication of

dx.doi.org/10.1021/jp311287t | J. Phys. Chem. B 2013, 117, 2061−2068

satellite features is observed in this system in contrast to a previously reported terpyridine complex.[6] In the studied WALP23 samples with almost 100% nitroxide labeling efficiency, we observe modulation depths of about 0.5 at X-band and about 0.3−0.4 at Q-band. This is in line with the values observed under comparable conditions in nitroxide−nitroxide DEER.[35] Thus the modulation depth in the Gd(III)−nitroxide DEER experiment with pumping on the nitroxide is not significantly influenced by the presence of high-spin Gd(III) centers. The large DEER modulation depth is a clear advantage of the presented pair of spin labels as it allows working with partially labeled samples, as they usually occur in bioapplications. Modulation depths in Gd(III)−Gd(III) DEER experiments at Q/Ka-band are typically an order of magnitude lower.[8,38,53,54] The distance distributions obtained from X- and Q-band data agree within the experimental error, in line with previous measurements and theoretical predictions.[6,8] The obtained distance distributions are in line with the expected α-helical structure of WALP23 and reveal an α-helix pitch close to the ideal value of 0.54 nm.

The spectroscopic selectivity for the Gd(III)−nitroxide pair with respect to nitroxide−nitroxide and Gd(III)−Gd(III) pairs is nearly perfect, mainly due to the difference in the transition moments for Gd(III) (S = 7/2) and nitroxide radicals (S = 1/2), leading to large difference in the optimal pulse settings.[6,8] This difference is an advantage compared to Cu(II)−nitroxide pairs with both spins 1/2,[55,56] where the optimal power settings are the same for both species. The expected spectroscopic selectivity in Mn(II)−nitroxide pairs should be somewhat worse than in Gd(III)−nitroxide pairs due to the lower spin of Mn^{2+} ion (S = 5/2), but it should be better than in Cu(II)−nitroxide pairs. An additional disadvantage of using Mn(II)-containing tags is the sensitivity loss, because of the splitting of the intensity of the central transition of Mn(II) into six hyperfine components.[57]

An important advantage of using spectroscopically orthogonal spin labels, as compared to the conventional nitroxide labeling, is the possibility of additional checks on each type of paramagnetic centers. We have demonstrated this on two examples: first, on the nitroxide mobility measurements, and second, on the measurements of the polypeptide agglomeration via nitroxide−nitroxide DEER. Clearly, more such options exist, and they are expected to be valuable in studies of complex biochemical systems.

These spectroscopic advantages can be especially valuable for EPR-based studies of protein aggregation,[58−60] protein−protein interactions, and folding.[61−65] In particular, the problem of peptide aggregation and incorporation into lipid bilayers is very important for antimicrobial properties of certain classes of peptides,[66−68] and this issue has been studied in detail by EPR techniques,[69,70] among them nitroxide−nitroxide DEER (PELDOR).[71−74]

Regarding additional checks on each of the two spin probes, one has to mention that the influence of the local environment on the spectroscopic parameters of Gd(III) centers has been studied to much less extent as compared to nitroxide spin probes.[11] The most relevant set of data has been obtained from pulse hyperfine spectroscopy on Gd(III) chelate complexes used in MRI,[46] where the main focus was on the hyperfine interaction with protons from water molecules directly bound to the Gd(III) ions. Studies on the influence of mobility, local polarity, pH, etc., on EPR parameters of Gd(III) centers now gain further importance, as they can help in broadening the applicability range of the Gd(III)−nitroxide orthogonal labeling approach.

A challenge for experiments with spectroscopically orthogonal spin labels attached to biomacromolecules is the labeling step. In some cases, such as studies of macromolecular complexes or protein−substrate or protein−cofactor interactions, different spin labels could be attached to different types of macromolecules. In cases when a single subunit of a biomacromolecular complex or a single biomacromolecule has to be labeled with two spectroscopically orthogonal tags, special labeling schemes have to be developed. A few approaches of this kind can be constructed by combining some lanthanide specific binding scheme, as for instance, an engineered lanthanide binding site[75] with a cysteine chemistry approach[11] for nitroxide attachment. Alternatively an unnatural amino acid-based approach[76] could be used for nitroxide attachment, whereas the lanthanide tags could be then attached to cysteine sites with the help of methane thiosulfonate or other thiol-specific groups. A proposed approach of randomly labeling cysteine sites with the two labels[14] gives up control on the site to which each type of label is attached, thus disallowing for checks on intermolecular interaction (aggregation) or local label environment. Further development of orthogonal labeling approaches is thus essential for the broad applicability of the presented technique. We currently study the performance of an unnatural amino acid-based approach[76] for orthogonal attachment of Gd(III) and nitroxide spin labels.

5. CONCLUSIONS

DEER distance measurements between spectroscopically orthogonal Gd(III) and nitroxide spin labels in the nanometer range have been performed for a series of peptides incorporated into a lipid bilayer. With bulk peptide concentrations between 85 and 260 μM, high signal-to-noise ratio DEER traces with lengths between 2 and 3 μs could be measured at both X- and Q-band frequensies, demonstrating sensitivity that is comparable to nitroxide−nitroxide DEER on lipid bilayer embedded biomacromolecules. The distance distributions obtained in X- and Q-band experiments agree and exhibit the expected shift of the mean distance by the α-helical pitch when the nitroxide labeling site is shifted by four residues, thus showing the reliability of Gd(III)−nitroxide distance measurements. The orthogonal labeling approach allows for site-specific studies of the nitroxide environment by pulse and CW EPR in the presence of the lanthanide label and for an independent check of aggregation within the lipid bilayer by nitroxide−nitroxide DEER measurements. The new approach could thus become a valuable complement to existing labeling-based distance measurement methods, provided that efficient labeling procedures for typical application scenarios are developed. Work along this line is now in progress.

■ ASSOCIATED CONTENT

Supporting Information

Transverse relaxation of Gd(III) centers; estimates of the ZFS parameters for the Gd(III)−DOTA label; DEER echo reduction effect. This material is available free of charge via the Internet at http://pubs.acs.org.

■ AUTHOR INFORMATION

Corresponding Author

* E-mail: maxim.yulikov@phys.chem.ethz.ch.

Notes

The authors declare no competing financial interest.

■ ACKNOWLEDGMENTS

We acknowledge financial support by the SNF (Grant No. 200021_121579) and by the European Community Activity Large-Scale Facility Wageningen NMR Center (FP6-2004-026164 (2006−2009)).

■ ABBREVIATIONS

MTSSL, *S*-(2,2,5,5-tetramethyl-2,5-dihydro-1*H*-pyrrol-3-yl)-methyl methanesulfonothioate spin label; DOTA, 1,4,7,10-tetraazacyclododecane-1,4,7,10-tetraacetic acid; DOPC, 1,2-dioleoyl-*sn*-glycero-3-phosphocholine; TFE, trifluoroethanol

■ REFERENCES

(1) Milov, A. D.; Salikhov, K. M.; Shirov, M. D. *Fiz. Tverd. Tela (Leningrad)* **1981**, *23*, 957−982. Milov, A. D.; Ponomarev, A. B.; Tsvetkov, Yu. D. *Chem. Phys. Lett.* **1984**, *110*, 67−72.
(2) Martin, R. E.; Pannier, M.; Diederich, F.; Gramlich, V.; Hubrich, M.; Spiess, H. W. *Angew. Chem., Int. Ed. Engl.* **1998**, *37*, 2834−2837. Pannier, M.; Veit, S.; Godt, A.; Jeschke, G.; Spiess, H. W. *J. Magn. Reson.* **2000**, *142*, 331−340.
(3) Saxena, S.; Freed, J. H. *Chem. Phys. Lett.* **1996**, *251*, 102−110. Borbat, P. P.; Freed, J. H. *Chem. Phys. Lett.* **1999**, *313*, 145−154.
(4) Kulik, L. V.; Dzuba, S. A.; Grigoryev, I. A.; Tsvetkov, Yu. D. *Chem. Phys. Lett.* **2001**, *343*, 315−324. Zaripov, R. B.; Dzhabarov, V. I.; Knyazev, A. A.; Galyametdinov, Yu. G.; Kulik, L. V. *Appl. Magn. Reson.* **2011**, *40*, 11−19.
(5) Milikisyants, S.; Scarpelli, F.; Finiguerra, M. G.; Ubbink, M.; Huber, M. *J. Magn. Reson.* **2009**, *201*, 48−56.
(6) Lueders, P.; Jeschke, G.; Yulikov, M. *J. Phys. Chem. Lett.* **2011**, *2*, 604−609.
(7) Maryasov, A. G.; Bowman, M. K.; Tsvetkov, Yu. D. *Appl. Magn. Reson.* **2006**, *30*, 683−702.
(8) Yulikov, M.; Lueders, P.; Warsi, M. F.; Chechik, V.; Jeschke, G. *Phys. Chem. Chem. Phys.* **2012**, *14*, 10732−10746.
(9) Jeschke, G.; Polyhach, Ye. *Phys. Chem. Chem. Phys.* **2007**, *9*, 1895−1910.
(10) Schiemann, O.; Prisner, T. F. *Q. Rev. Biophys.* **2007**, *40*, 1−53.
(11) Bordignon, E. *Curr. Top. Chem.* **2012**, *321*, 121−157.
(12) Krstić, I.; Edenward, B.; Margraf, D.; Marko, A.; Prisner, T. *Curr. Top. Chem.* **2012**, *321*, 159−198.
(13) Jeschke, G. *Annu. Rev. Phys. Chem.* **2012**, *63*, 419−446.
(14) Kaminker, I.; Yagi, H.; Huber, T.; Feintuch, A.; Otting, G.; Goldfarb, D. *Phys. Chem. Chem. Phys.* **2012**, *14*, 4355−4358.
(15) Su, X.-C.; Otting, G. *J. Biomol. NMR* **2010**, *46*, 101−112.
(16) Keizers, P. H. J.; Ubbink, M. *Prog. NMR Spectrosc.* **2011**, *58*, 88−96.
(17) Killian, J.; Salemink, I.; dePlanque, M.; Lindblom, G.; Koeppe, R.; Greathouse, D. *Biochemistry* **1996**, *35*, 1037−1045.
(18) Morein, S.; Strandberg, E.; Killian, J.; Persson, S.; Arvidson, G.; Koeppe, R.; Lindblom, G. *Biophys. J.* **1997**, *73*, 3078−3088.
(19) de Planque, M.; Goormaghtigh, E.; Greathouse, D.; Koeppe, R.; Kruijtzer, J.; Liskamp, R.; de Kruijff, B.; Killian, J. *Biochemistry* **2001**, *40*, 5000−5010.
(20) Killian, J. *Biochim. Biophys. Acta, Rev. Biomembr.* **1998**, *1376*, 401−416.
(21) Lueders, P.; Jäger, H.; Hemminga, M. A.; Jeschke, G.; Yulikov, M. *J. Phys. Chem. Lett.* **2012**, *3*, 1336−1340.
(22) Jäger, H.; Koch, A.; Maus, V.; Spiess, H.; Jeschke, G. *J. Magn. Reson.* **2008**, *194*, 254−263.
(23) Nielsen, R.; Che, K.; Gelb, M.; Robinson, B. *J. Am. Chem. Soc.* **2005**, *127*, 6430−6442.
(24) Su, X.-C.; Otting, G. *J. Biomol. NMR* **2010**, *46*, 101−112.
(25) Keizers, P. H. J.; Ubbink, M. *Prog. NMR Spectrosc.* **2011**, *58*, 88−96.
(26) Liu, Y.; Nagle, J. F. *Phys. Rev. E* **2004**, *69*, 040901(R).
(27) Tristram-Nagle, S.; Petrache, H. I.; Nagle, J. F. *Biophys. J.* **1998**, *75*, 917−925.
(28) Wang, X. Y.; Jin, T.; Comblin, V.; Lopez-Mut, A.; Merciny, E.; Desreux, J. F. *Inorg. Chem.* **1992**, *31*, 1095−1099.
(29) Prosser, R. S.; Hunt, S. A.; DiNatale, J. A.; Vold, R. R. *J. Am. Chem. Soc.* **1996**, *118*, 269−270. Prosser, R. S.; Bryant, H.; Bryant, R. G.; Vold, R. R. *J. Magn. Reson.* **1999**, *141*, 256−260.
(30) Gromov, I.; Shane, J.; Forrer, J.; Rakhmatoullin, R.; Rozentzwaig, Y.; Schweiger, A. *J. Magn. Reson.* **2001**, *149*, 196−203.
(31) Tschaggelar, R.; Kasumaj, B.; Santangelo, M. G.; Forrer, J.; Leger, P.; Dube, H.; Diederich, F.; Harmer, J.; Schuhmann, R.; García-Rubio, I.; et al. *J. Magn. Reson.* **2009**, *200*, 81−87.
(32) Tsvetkov, Yu. D.; Grishin, Yu. A. *Instrum. Exp. Tech.* **2009**, *52*, 615−636.
(33) Tkach, I.; Sicoli, G.; Höbartner, C.; Bennati, M. *J. Magn. Reson.* **2011**, *209*, 341−346.
(34) Cruickshank, P. A. S.; Bolton, D. R.; Robertson, D. A.; Hunter, R. I.; Wylde, R. J.; Smith, G. M. *Rev. Sci. Instrum.* **2009**, *80*, 103102.
(35) Polyhach, Y.; Bordignon, E.; Tschaggelar, R.; Gandra, S.; Godt, A.; Jeschke, G. *Phys. Chem. Chem. Phys.* **2012**, *14*, 10762−10773.
(36) Ghimire, H.; McCarrick, R. M.; Budil, D. E.; Lorigan, G. A. *Biochemistry* **2009**, *48*, 5782−5784.
(37) Zou, P.; Mchaourab, H. S. *Biophys. J.* **2010**, *98*, L18−L20.
(38) Raitsimring, A. M.; Gunanathan, C.; Potapov, A.; Efremenko, I.; Martin, J. M. L.; Milstein, D.; Goldfarb, D. *J. Am. Chem. Soc.* **2007**, *129*, 14138−14139. Gordon-Grossman, M.; Kaminker, I.; Gofman, Y.; Shai, Y.; Goldfarb, D. *Phys. Chem. Chem. Phys.* **2011**, *13*, 10771−10780.
(39) Jeschke, G.; Chechik, V.; Ionita, P.; Godt, A.; Zimmermann, H.; Banham, J.; Timmel, C. R.; Hilger, D.; Jung, H. *Appl. Magn. Reson.* **2006**, *30*, 473−498, http://www.epr.ethz.ch/software/index.
(40) Tikhonov, A. N.; Arsenin, V. Y. *Solutions of Ill-Posed Problems*; John Wiley & Sons: New York, 1977.
(41) Jeschke, G.; Panek, G.; Godt, A.; Bender, A.; Paulsen, H. *Appl. Magn. Reson.* **2004**, *26*, 223−244.
(42) Chiang, Y. W.; Borbat, P. P.; Freed, J. H. *J. Magn. Reson.* **2005**, *172*, 279−295.
(43) Voss, J.; Wu, J.; Hubbell, W. L.; Jacques, V.; Meares, C. F.; Kaback, H. R. *Biochemistry* **2001**, *40*, 3184−3188.
(44) Raitsimring, A. M.; Astashkin, A. V.; Poluektov, O. G.; Caravan, P. *Appl. Magn. Reson.* **2005**, *28*, 281−295.
(45) Benmelouka, M.; Van Tol, J.; Borel, A.; Nellutla, S.; Port, M.; Helm, L.; Brunel, L.-C.; Merbach, A. E. *Helv. Chim. Acta* **2009**, *92*, 2173−2185.
(46) Raitsimring, A. M.; Astashkin, A. V.; Caravan, P. In *Biological Magnetic Resonance*; Hanson, G., Berliner, L. J., Eds.; Springer−Verlag: New York, 2009, *28*, 581−621.
(47) Bloch, F.; Siegert, A. *Phys. Rev.* **1940**, *57*, 522−527.
(48) Bowman, M. K.; Maryasov, A. G. *J. Magn. Reson.* **2007**, *185*, 270−282.
(49) Kaminker, I.; Yagi, H.; Huber, T.; Feintuch, A.; Otting, G.; Goldfarb, D. *Phys. Chem. Chem. Phys.* **2012**, *14*, 4355−4358.
(50) Jeschke, G. *Struct. Bonding (Berlin, Ger.)* **2011**, DOI: 10.1007/430_2011_61.
(51) Hubbell, W. L.; Cafiso, D. S.; Altenbach, C. *Nat. Struct. Biol.* **2000**, *7*, 735−739.
(52) Dastvan, R.; Bode, B. E.; Karuppiah, M. P. R.; Marko, A.; Lyubenova, S.; Schwalbe, H.; Prisner, T. F. *J. Phys. Chem. B* **2010**, *114*, 13507−13516.
(53) Potapov, A.; Song, Y.; Meade, T. J.; Goldfarb, D.; Astashkin, A. V.; Raitsimring, A. M. *J. Magn. Reson.* **2010**, *205*, 38−49.
(54) Song, Y.; Meade, T. J.; Astashkin, A. V.; Klein, E. L.; Enemark, J. H.; Raitsimring, A. *J. Magn. Reson.* **2011**, *210*, 59−68.
(55) Narr, E.; Godt, A.; Jeschke, G. *Angew. Chem., Int. Ed.* **2002**, *41*, 3907−3910.
(56) Yang, Z.; Kise, D.; Saxena, S. *J. Phys. Chem. B* **2010**, *114*, 6165−6174.

(57) Banerjee, D.; Yagi, H.; Huber, T.; Otting, G.; Goldfarb, D. *J. Phys. Chem. Lett.* **2012**, *3*, 157−160.
(58) Margittai, M.; Langen, R. *Methods Enzymol.* **2006**, *413*, 122−139.
(59) Apostolidou, M.; Jayasinghe, S. A.; Langen, R. *J. Biol. Chem.* **2008**, *283*, 17205−17210.
(60) Bedrood, S.; Li, Y.; Isas, J. M.; Hegde, B. G.; Baxa, U.; Haworth, I. S.; Langen, R. *J. Biol. Chem.* **2012**, *287*, 5235−5241.
(61) Lilly, A. A.; Crane, J. M.; Randall, L. L. *Protein Sci.* **2009**, *18*, 1860−1868.
(62) Cooper, D. B.; Smith, V. F.; Crane, J. M.; Roth, H. C.; Lilly, A. A.; Randall, L. L. *J. Mol. Biol.* **2008**, *382*, 74−87.
(63) Jun, S.; Becker, J. S.; Yonkunas, M.; Coalson, R.; Saxena, S. *Biochemistry* **2006**, *45*, 11666−11673.
(64) Fafarman, A. T.; Borbat, P. P.; Freed, J. H.; Kirshenbaum, K. *Chem. Commun.* **2007**, *4*, 377−379.
(65) Upadhyay, A. K.; Borbat, P. P.; Wang, J.; Freed, J. H.; Edmondson, D. E. *Biochemistry* **2008**, *47*, 1554−1566.
(66) Makovitzki, A.; Baram, J.; Shai, Y. *Biochemistry* **2008**, *47*, 10630−10636.
(67) Toniolo, C.; Crisma, M.; Formaggio, F.; Peggion, C.; Epand, R. F.; Epand, R. M. *Cell. Mol. Life Sci.* **2001**, *58*, 1179−1188.
(68) Stella, L.; Mazzuca, C.; Venanzi, M.; Palleschi, A.; Didone, M.; Formaggio, F.; Toniolo, C.; Pispisa, B. *Biophys. J.* **2004**, *86*, 936−945.
(69) Salnikov, E. S.; De Zotti, M.; Formaggio, F.; Li, X.; Toniolo, C.; O'Neil, J. D. J.; Raap, J.; Dzuba, S. A.; Bechinger, B. *J. Phys. Chem. B* **2009**, *113*, 3034−3042.
(70) Syryamina, V. N.; Isaev, N. P.; Peggion, C.; Formaggio, F.; Toniolo, C.; Raap, J.; Dzuba, S. A. *J. Phys. Chem. B* **2010**, *114*, 12277−12283.
(71) Milov, A. D.; Tsvetkov, Yu. D.; Formaggio, F.; Crisma, M.; Toniolo, C.; Raap, J. *J. Pept. Sci.* **2003**, *9*, 690−700.
(72) Milov, A. D.; Erilov, D. A.; Salnikov, E. S.; Tsvetkov, Yu. D.; Formaggio, F.; Toniolo, C.; Raap, J. *Phys. Chem. Chem. Phys.* **2005**, *7*, 1794−1799.
(73) Salnikov, E. S.; Erilov, D. A.; Milov, A. D.; Tsvetkov, Yu. D.; Peggion, C.; Formaggio, F.; Toniolo, C.; Raap, J.; Dzuba, S. A. *Biophys. J.* **2006**, *91*, 1532−1540.
(74) Milov, A. D.; Samoilova, R. I.; Tsvetkov, Yu. D.; De Zotti, M.; Formaggio, F.; Toniolo, C.; Handgraaf, J.-W.; Raap, J. *Biophys. J.* **2009**, *96*, 3197−3209.
(75) Jia, X.; Yagi, H.; Su, X.-C.; Stanton-Cook, M.; Huber, T.; Otting, G. *J. Biomol. NMR* **2011**, *50*, 411−420.
(76) Fleissner, M. R.; Brustad, E. M.; Kálai, T.; Altenbach, C.; Cascio, D.; Peters, F. B.; Hideg, K.; Peuker, S.; Schultz, P. G.; Hubbell, W. L. *Proc. Natl. Acad. Sci. U.S.A.* **2009**, *106*, 21637−21642.